BEST AVAILABLE IMAGES

Defective images within this document are accurate representations of the original documents submitted by the applicant.

Defects in the images may include (but are not limited to):

- BLACK BORDERS
- TEXT CUT OFF AT TOP, BOTTOM OR SIDES
- FADED TEXT
- ILLEGIBLE TEXT
- SKEWED/SLANTED IMAGES
- COLORED PHOTOS
- BLACK OR VERY BLACK AND WHITE DARK PHOTOS
- GRAY SCALE DOCUMENTS

IMAGES ARE BEST AVAILABLE COPY.

As rescanning documents *will not* correct images, please do not report the images to the Image Problem Mailbox.

ELSEVIER

European Journal of Pharmaceutical Sciences 11 (2000) 191–198

EUROPEAN JOURNAL OF PHARMACEUTICAL SCIENCES

www.elsevier.nl/locate/ejps

Mini Review

Rational selection of antisense oligonucleotide sequences

Lise Smith[a], Klaus Bahl Andersen[b], Lars Hovgaard[a,*], Jerzy W. Jaroszewski[c]

[a]*Department of Pharmaceutics, The Royal Danish School of Pharmacy, Universitetsparken 2, DK-2100 Copenhagen, Denmark*
[b]*Department of Pharmacology, The Royal Danish School of Pharmacy, Universitetsparken 2, DK-2100 Copenhagen, Denmark*
[c]*Department of Medicinal Chemistry, The Royal Danish School of Pharmacy, Universitetsparken 2, DK-2100 Copenhagen, Denmark*

Received 4 October 1999; received in revised form 13 April 2000; accepted 25 April 2000

Abstract

The purpose of this review is to identify rational selection procedures for the identification of optimal antisense oligonucleotide sequences. The review is firstly focused on how to find optimal hybridization sites, and secondly on how to select sequences that bind to structured RNA. The methods reviewed range from the more empirical testing of large numbers of mRNA complementary sequences to the more systematic techniques, i.e. RNase H mapping, use of combinatorial arrays and prediction of secondary structure of mRNA by computational methods. Structures that bind to structured RNA, i.e. aptastrucs and tethered oligonucleotide probes, and foldback triplex-forming oligonucleotides are also discussed. Relating to selection of antisense sequences by aid of computational analysis, valuable www addresses are given along with examples of folded structures of mRNA.

Keywords: Antisense oligonucleotides; Antisense selection; mRNA targeting; mRNA secondary structure; Mfold

1. Introduction

Antisense oligonucleotides inhibit translation of mRNA by various mechanisms. They can cause translational arrest by hybridizing to mRNA at binding sites for ribosomes (Uhlmann and Peyman, 1990). The target sites for this mechanism are the AUG codon or the 5′ untranslated region (Jaroszewski, 1998). Another important mechanism is RNase H activation, in which RNase H cleaves the RNA strand of an RNA–DNA duplex (Uhlmann and Peyman, 1990). Any sequence within the mRNA can be a target for this mechanism of antisense inhibition (Jaroszewski, 1998). Furthermore, antisense oligonucleotides can be targeted to splicing sites inhibiting the production of mature mRNA or to the capping and polyadenylation sites causing destabilization of the mRNA (Crooke, 1995a). For reviews on the mechanisms of action of oligonucleotides, see Crooke (1995a) and Uhlmann and Peyman (1990).

The potency of antisense oligonucleotides varies substantially and is dependent on the mechanism of action, the secondary structure of mRNA and characteristics of the oligonucleotides (Crooke, 1995b). The best target site is not easily predictable; therefore, it is imperative to search for optimal target sequences using oligonucleotides acting by different mechanisms, having different affinities and characteristics (Crooke, 1995b).

In order to increase the success rate of selecting antisense oligonucleotide sequences, many attempts have been made to find rational selection procedures (Table 1). The purpose of this review is to provide an overview of these methods that will enable a better selection of antisense sequences.

1.1. Finding optimal hybridization sites in the target mRNA

Optimal hybridization sites can be found by empirical testing or by finding accessible sites in the mRNA by a variety of methods.

1.1.1. 'Walk the gene'

The traditional way of selecting antisense oligonucleotide sequences has been to 'walk the gene', i.e. empirically test a large number (up to 50) of sequences complementary to various sites in the target mRNA in order to find the most potent sequence. Indeed, some research groups have succeeded in finding the needle in the haystack. An example is the discovery of a very potent antisense inhibitor targeted against C-*raf* kinase mRNA, where one

*Corresponding author. Tel.: +45-35-306-370; fax: +45-35-306-030.
E-mail address: lh@dfh.dk (L. Hovgaard).

0928-0987/00/$ – see front matter
PII: S0928-0987(00)00100-7

Table 1
Rational selection procedures for antisense oligonucleotides

Selection procedure	References
Finding optimal hybridization sites in the target mRNA	
'Walk the gene'	Monia et al., 1996; Akhtar, 1998
RNase H mapping of accessible sites	Ho et al., 1996, 1998; Bruice and Lima, 1997; Lima et al., 1997; Matveeva et al., 1997
Combinatorial oligonucleotide array on solid support	Southern et al., 1994; Milner et al., 1997
Determination of secondary structure by enzymatic mapping	Lima et al., 1992
Secondary structure analysis by computational methods	Jaroszewski et al., 1993; Sczakiel et al., 1993; Patzel et al., 1997; Patzel and Sczakiel, 1998; Sohail et al., 1999
Selection of sequences that bind to structured RNA	
Aptastrucs	Mishra and Toulmé, 1994; Mishra et al., 1996; Le Tinévez et al., 1998
Tethered oligonucleotide probes	Cload and Schepartz, 1994
Foldback triplex-forming oligonucleotides	Kandimalla and Agrawal, 1994
Selection of sequences with minimized non-specific binding	Han et al., 1994; Mitsuhashi et al., 1994
Empirically found targets	Tu et al., 1998

of 34 phosphorothioate oligonucleotides showed more than 90% inhibition, and only four showed more than 70% inhibition, whereas 16 showed less than 10% inhibition at 200 nM in cultured tumor cells (Monia et al., 1996). As illustrated, to 'walk the gene' is a lengthy procedure, the success of which is based on a great deal of luck, as it is not practical to test all possible sequences (Akhtar, 1998).

1.1.2. RNase H mapping

A highly promising strategy for selection of antisense oligonucleotide sequences is RNase H mapping of accessible sites within the target mRNA (Fig. 1). The principle of this selection procedure is that a random or semi-random library of oligonucleotides is allowed to hybridize with mRNA, and the DNA–RNA hybrid is digested with RNase H. Sequences of the resulting fragments are analyzed to locate the accessible sites. Oligonucleotides are then selected towards the cleavage sites (Ho et al., 1996, 1998; Bruice and Lima, 1997; Lima et al., 1997; Matveeva et al., 1997). Phosphorothioate or chimeric oligonucleotides targeted to the accessible sites found in an RNase H mapping experiment were highly active (>80% inhibition) in cellular antisense experiments in five of six cases (Ho et al., 1996). When testing thirteen 20-mer 'walking oligonucleotides' covering 200 nt of the h*MDR1* mRNA with 5 nt overlaps, only three showed more than 70% inhibition. In another study from the same group, oligonucleotides targeted to every accessible site found by RNase H mapping were shown to be active (Ho et al., 1998). The authors tried to correlate results from RNase H mapping with computational prediction of RNA secondary structure, but no significant differences were found between the structure of the regions targeted by active versus inactive oligonucleotides (Ho et al., 1998). This indicates that RNase H mapping may be a better selection procedure as compared to secondary structure prediction. Bruice and Lima found a direct correlation of antisense inhibition with hybridization affinity in an RNase H cleavage assay using a completely random 10-mer oligonucleotide library (Lima et al., 1997). An earlier attempt to use a random library in a hybridization assay using RNase ONE failed at least in part due to the occurrence of self-complementary oligonucleotides in the random library (Bruice and Lima, 1997). Replacing the RNase ONE, which cleaves the single-stranded sequences with RNase H that cleaves the much less frequent RNA–DNA duplexes, led to better results.

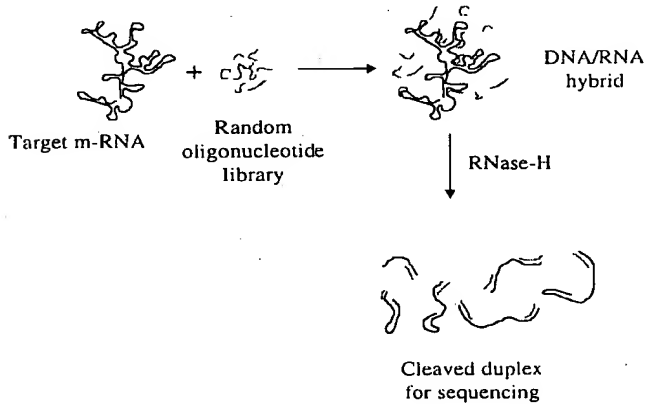

Fig. 1. Schematic representation of RNase H mapping of duplex formation targets in mRNA. A random ODN library is allowed to hybridize and subsequently cleaved by RNase H. Fragments are sequence analyzed to identify the targets.

Matveeva et al. (1997) suggested a modified RNase H mapping procedure. In this procedure, RNA was transcribed from a PCR-amplified DNA region. A random

pool of complementary DNA fragments of 10–50 bp was prepared by DNase digestion of the DNA used to synthesize the target RNA. The DNA fragments were denatured, hybridized with target RNA and the hybrids were cleaved by RNase H. A correlation between antisense effect in a cell culture and the accessible sites identified by this method was shown. Further, the method should be quicker than those mentioned above because it does not require oligonucleotide synthesis, and because large RNA sequences can be analyzed.

A limitation of the RNase H mapping procedure for selection of antisense oligonucleotides might be that some RNA sites accessible for oligonucleotide hybridization could be overlooked due to steric inaccessibility to RNase H (Lima et al., 1997). On the other hand, it is indeed highly relevant to use RNase H cleavage as a selection procedure, because the RNase H mechanism is important to the antisense effect in cell cultures and in vivo (Ho et al., 1998).

1.1.3. Combinatorial oligonucleotide array on solid support

In this technique, all possible antisense oligonucleotide sequences up to a chosen maximum length, targeting a certain mRNA, are synthesized on a solid support, e.g. glass plate (Southern et al., 1994) (Fig. 2). Coupling is carried out using a reaction chamber, in which the reagents are applied in a well-defined area. The length of oligonucleotides is elegantly controlled by the dimensions of the reaction chamber and the size of the steps by which the reaction chamber is displaced before the next coupling step takes place. Hybridization between the combinatorial oligonucleotide array and, for example, radioactively labeled target mRNA determines the site for optimal hybridization. Duplex yield determined by the combinatorial array method correlated well with antisense activity in vitro as well as with RNase H cleavage results (Milner et al., 1997). On the other hand, the optimal sites for hybridization could not be recognized by secondary structure analysis. Milner et al. (1997) suggested that RNase H mapping could be used as the first screening for accessible sites in target mRNA, and hybridization with combinatorial arrays could then be used to find the best site for optimal hybridization among the accessible sites.

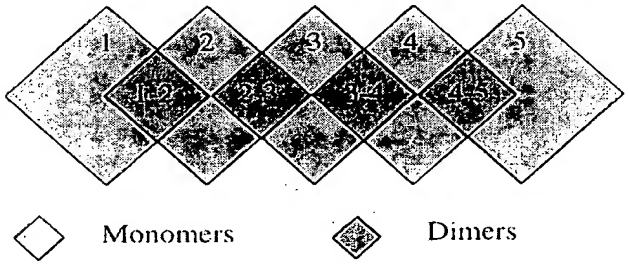

Fig. 2. Simplified representation of the construction of ODN arrays on solid support. The example illustrates the formation of a 2-mer. For more detailed illustration, see Southern et al. (1994).

1.1.4. Determination of secondary structure by enzymatic mapping

The structure of RNA can be determined by enzymatic mapping, in which specific enzymes are utilized to cleave specific structures. In this way, information about the full structure is collected. Enzymatic structure mapping of a 47 nt transcript employing RNase T1, V1, CL3, A and S1 digestion revealed a stable hairpin structure (Lima et al., 1992). As expected, a stronger hybridization was observed for antisense oligonucleotides targeted to the loop than for those targeted to the stem of the hairpin. However, not all single-stranded regions were good targets due to steric hindrance of the RNases. As a way of selecting antisense oligonucleotide sequences, this method seems only feasible for relatively short transcripts, whereas enzymatic probing of a full length mRNA of perhaps a thousand bases would be very laborious.

1.1.5. Secondary structure analysis by computational methods

The program Mfold (Mathews et al., 1999; Zuker et al., 1999) predicts the secondary structure of RNA based on free energy minimization. The program calculates the global free energy minimum of an RNA molecule based on thermodynamic data for the formation of base pairs and structural features such as helices and loops. Mfold calculates the optimal structure and an optional number of suboptimal structures. Statistical analysis of the predicted structures can then be carried out in order to identify predominantly single-stranded and predominantly double-stranded regions in mRNA. The intrinsic weakness of this method is the treatment of a mRNA molecule as an isolated species. The method does not take into account external factors, i.e. interaction with cytoplasmic components (metal ions and proteins). Moreover, a possible tertiary structure is not taken into account.

In an attempt to rationally select antisense oligonucleotides against mRNA from the pQBI63 plasmid coding for rsGFP (red shift Green Fluorescent Protein) we have used the following strategy. By use of the Mfold program it is possible to create folded low-energy secondary structures (Figs. 3 and 4) (Mfold versions 2.3 and 3.0; Zuker et al., 1999). The program is available at the Mfold server ©1995–2000, Michael Zuker, Washington University School of Medicine, 'http://mfold2.wustl.edu/~mfold/rna/form1.cgi'. Based on these structures a number of possible antisense oligonucleotide sequences can be selected. Then in order to minimize the risk of self-hybridization or hairpin formation the program Quickfold 'http://mfold.wustl.edu/folder/rna/form3.cgi' on the Mfold server is useful for verifying that the sequences selected do not fold back on themselves. The theoretical melting point, which is of importance for the hybridization intensity in the

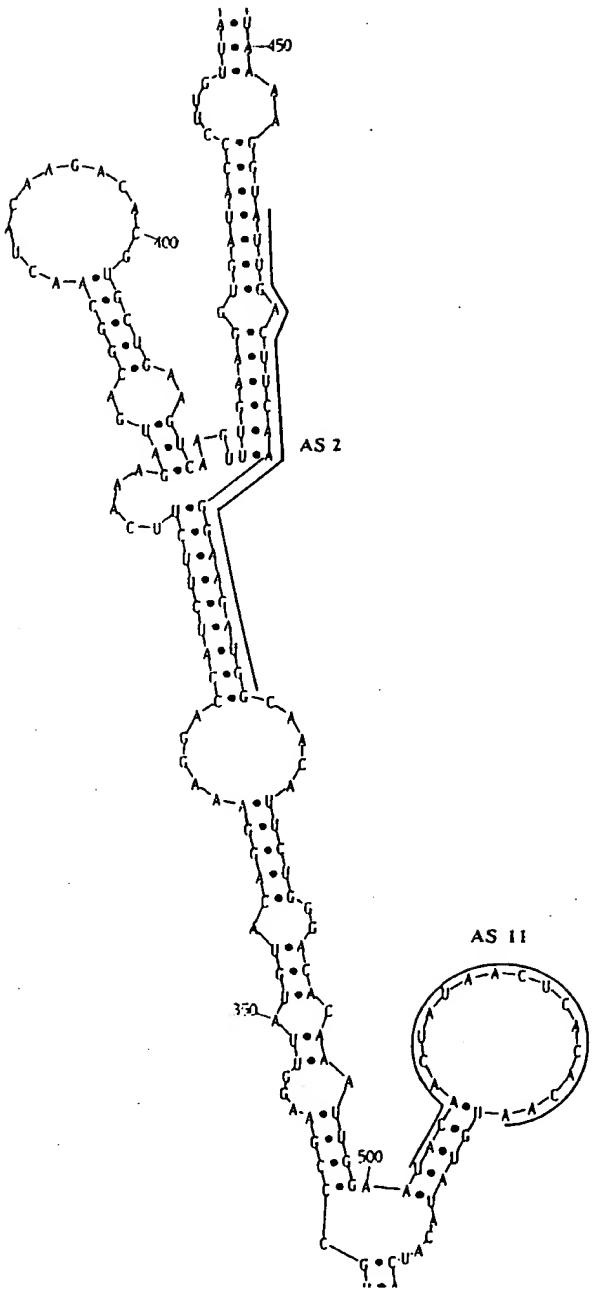

Fig. 3. Shown is a fragment of the optimal secondary structure of rsGFP mRNA at 30°C as calculated by Mfold 2.3. The target sequences for two of the selected antisense oligonucleotide sequences are indicated. AS 2 is targeting a highly folded region of the mRNA and AS 11 is targeting a single-stranded region. AUG is base 73–75.

DNA–RNA duplexes, can be obtained from the Molecular Neurobiology homepage, Institut Pasteur, France, 'http://www.pasteur.fr/recherche/unites/neubiomol/meltinghome.html', where the program Melting4 is available (Le Novère, 2000). Finally, to ensure that the oligonucleotide sequences do not dimerize, the Lalign program on the Genestream network server, IGH Montpellier, France, 'http://vega.igh.cnrs.fr/bin/lalign-guess.cgi' can be used. All mentioned web addresses were last visited and confirmed on April 10, 2000. Table 2 shows a set of oligonucleotide sequences selected and tested in this manner. Future studies will show if the selection methods correlate with the biological activity of the compounds.

In order to evaluate the predictability of Mfold calculations, folding of different 16S mRNAs with well-known secondary structures were performed. The prediction varied for different RNAs (Zuker and Jacobson, 1995). The correspondence between the known and predicted structures ranged from 27 to 70%, with a mean value of 49%. The identity between the known and predicted structures improved to 81% when the analysis was limited to well-determined helices, i.e. structural domains in the predicted structure that were well preserved for all suboptimal structures calculated. This indicates that one should be careful when relying on a calculated structure if there is a large extent of flexibility in the structure, shown by large differences in the suboptimal structures calculated. Recently (Mathews et al., 1999), the algorithm employed to calculate the secondary structure was refined with new experimental data for the thermodynamic parameters used. It was found that the predicted lowest free energy structure contained, on average, 73% of the known base-pairs when less than 700 nt was folded. Consequently, the reliability of the calculations decreases with increased length of mRNA.

The Mfold 2.0 program was used to find the 30 low-energy structures of rabbit β-globin mRNA (589 bases) (Jaroszewski et al., 1993), which were found to be highly double-stranded. The computer predictions were consistent with nuclease digestion results found in the literature (Pavlakis et al., 1980). Antisense oligonucleotides were designed against targets with different degrees of double-strandedness and these oligonucleotides were tested in in vitro translations with wheat germ extract (WGE) and rabbit reticulocyte lysate (RRL). A linear correlation (r^2 = 0.95) was found between percentage of translation inhibition and percentage of unpaired target for translation with WGE, which is rich in RNase H, whereas no correlation was observed for translation with RRL, where RNase H activity was absent. The authors suggested that mRNA folding analysis could be used for selection of oligonucleotides in cases where RNase H mediated translation inhibition is the predominant inhibition mechanism (Jaroszewski et al., 1993).

In a recent study, transcripts of varying length (175, 336, 512, 1291 and 1389 nt) were hybridized with an oligonucleotide array targeting 111 nt from position 114–224 in the mRNA for cyclin B5 (Sohail et al., 1999). Similarities in hybridization patterns were observed and some features seen in the hybridization with short tran-

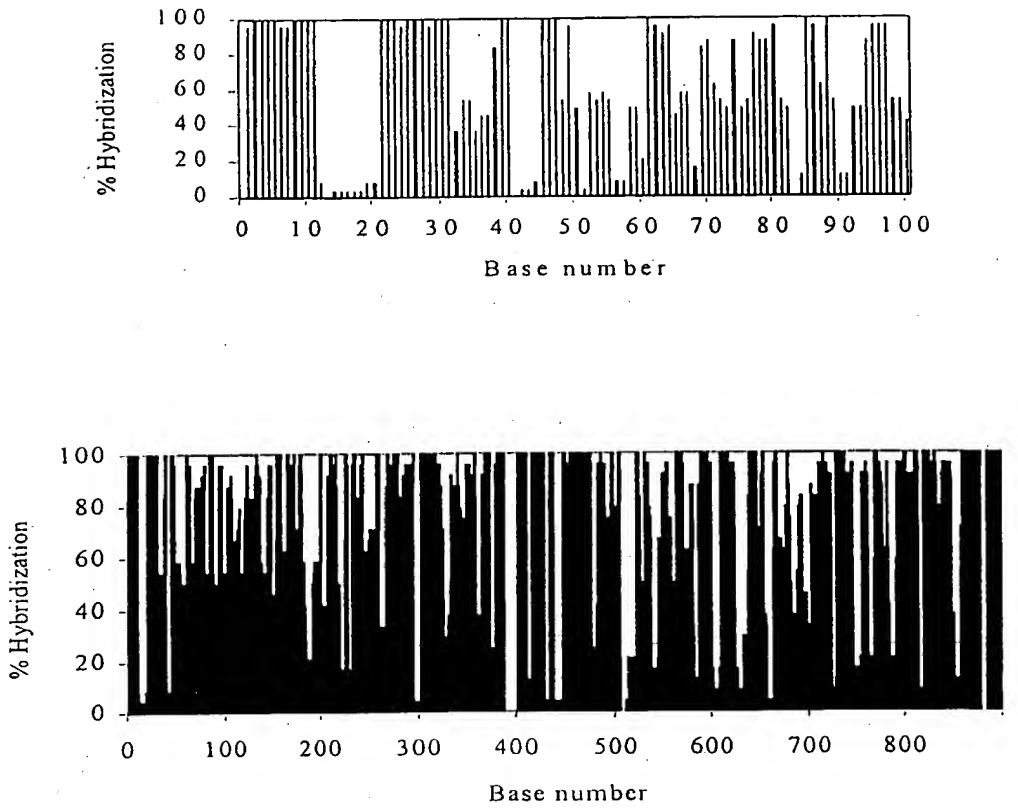

Fig. 4. Folding of rsGFP mRNA. Shown here, for each base position, is the percentage of structures in which the particular base is involved in intramolecular hybridization. Enlarged is shown the region from base 1 to 100. AUG is base 73–75.

scripts were not observed in the hybridization with the long transcripts. The strongest hybridization pattern was however preserved in the foldings of all transcripts. Predictions of structures by Mfold showed different structures for the RNA of different sizes with few structural parts shared between the structures. If folding by Mfold and hybridization should correlate well, the preserved area of hybridization should be shown to be accessible by RNA folding prediction for all the foldings. The best correlation between hybridization and secondary structure prediction was observed for the 175 nt transcript. This transcript represents an early stage of transcription. That the foldings of the longer transcripts fit badly with hybridization indicates that local foldings established early in transcription persist to a large extent throughout transcription and that large RNA probably do not reach a global minimal free energy structure, which is the structure found by Mfold. According to this study the use of secondary structure predictions have limited value in the design of antisense oligonucleotides (Sohail et al., 1999).

The secondary structure of different HIV-1-directed antisense RNA species of approximately 100 nt was calculated by Mfold 2.0 (Patzel et al., 1997; Patzel and Sczakiel, 1998). The calculated secondary structures of HIV-1-directed antisense RNA were in agreement with enzymatic probing by RNase T1 and RNase A. Moreover, the annealing rate between antisense RNA and the target RNA was measured in vitro and was found to be consistent with the number of terminal external bases (i.e., single-stranded ends) found by computational folding analysis (Foldanalyze). There was a good correlation between fast annealing (and thereby the number of terminal external bases) and antisense effect (inhibition of HIV-1 replication). The same correlation between predicted secondary structure, fast-annealing and antisense effect was also demonstrated for various antisense oligodeoxynucleotide sequences (Patzel et al., 1997). Low local folding potential (high local free energy, ΔG) of the target sequence indicating a single-stranded structure was found to be favorable but not sufficient for fast RNA–RNA annealing (Patzel et al., 1997). The free energy of folded RNA segments of length 50–400 nt of the HIV-1 genome was calculated by the program Husar (Sczakiel et al., 1993). The energy profile was compared with the effect of HIV-1-directed antisense RNAs. Significant minima of the local folding potential (high ΔG values) correlated well with regions where strong antisense inhibition was observed. Antisense RNAs targeting regions with a high folding

Table 2
Predicted characteristics of antisense oligonucleotides targeted to rsGFP mRNA selected by secondary structure computational analysis using *Mfold, Quickfold, Melting and Lalign*

Code	Target bases in mRNA[a]	Hybridization of target (%)	Antisense sequence (5′–3′)	GC content	T_m of ON-mRNA (°C)	Hairpin formation[c] Bp	Hairpin formation[c] T_m	Self-hybridizing strand in oligonucleotide[d] Bases	Self-hybridizing strand in oligonucleotide[d] T_m[e]	Other targets in mRNA[f] %[g]	Other targets in mRNA[f] Bases	Other targets in mRNA[f] T_m
AS 1	624–643	40	CGC CAA TTG GAG TAT TTT GT	40	56	2	36	8	21	73.3	15	16
AS 2	457–476	92	CCA TCT TCC TTG AAG TCA AT	40	59	3	40	4	[h]	80.0	15	29
						4	39					
						3	32					
AS 3	56–75	59	CAT ATG TAT ATC TCC TTC TT	30	54			6	[h]	78.6	14	24
AS 4	66–85	62	CTT TGC TAG CCA TAT GTA TA	35	56			6	[h]	80.0	20	34
AS 5	12–31	57	AGG GGA ATT GTT ATC CGC TC	50	61	4	50	4	[h]	75.0	16	27
						5	46					
AS 6	20–39	78	ATT TCT AGA GGG GAA TTG TT	35	53			4	[h]	78.9	19	30
AS 8	21–40	83	TAT TTC TAG AGG GGA ATT GT	35	52			5	[h]	76.2	21	32
AS 9	41–60	44	TTC TTA AAG TTA AAC AAA AT	15	33			4	[h]	83.3	12	4
AS 10	705–724	85	GGT CTC TCT TTT CGT TGG GA	50	67			2	[h]	73.3	15	26
AS 11	502–521	26	TTG TGT GAG TTA TAG TTG TA	30	54			4	[h]	78.6	14	18
SCR 1	[b]		AGC TCG TGT TCC TAC TGA TG	50				3	[h]	88.9	9	24
SCR 2	[b]		TGC GAA CTT TTC AAT TGT TG	35		2	38	6	[h]	71.4	14	12
						3	30					

[a] AUG is base 73–75. The 5′UTR covers base 1–72, the AUG region covers base 56–92 and the coding region covers base 76–792.
[b] SCR 1 and SCR 2 are scrambled sequences.
[c] Number of basepairs (bp) involved in hairpin stem and T_m for hairpin (only hairpins with $T_m > 30$°C are stated).
[d] Only the longest strands are stated.
[e] T_m for the dimer is stated. If several strands exist with the same length, T_m for all these strands are stated.
[f] The sites with highest T_m of ON-mRNA hybrid are stated.
[g] Percentage of complementarity between oligonucleotide sequence and target sequence.
[h] No stable duplex formation at room temperature.

potential showed weak or no antisense effect in human cells (Sczakiel et al., 1993).

In conclusion, both failures and successes of the use of computational folding prediction of mRNA as an aid in antisense sequence design have been reported.

1.2. Selection of sequences that bind to structured RNA

The fact that mRNA is folded has been utilized to select antisense oligonucleotide sequences that bind to structured rather than to single-stranded RNA.

1.2.1. Aptastrucs

The term *aptastruc* was introduced for aptamer oligonucleotides targeted to structured nucleic acids (Mishra and Toulmé, 1994). Oligonucleotides were selected towards a model DNA hairpin. Candidates contained a hexamer complementary to the target, a site that forms a *Sac* I restriction site when bound to a 'selector' molecule, a primer extension site and a variable region. Selector molecules containing the *Sac* I site were used to destroy the candidates not bound to the target and the bound oligonucleotides were amplified by PCR (Mishra and Toulmé, 1994; Mishra et al., 1996). The hexamers alone were not able to hybridize with the DNA hairpin efficiently. Nor were the variable regions themselves. The interactions could not be explained by primary sequences, as there was no complementarity. The oligonucleotides bind therefore to the secondary structure of their target by non-canonical base pairing. When these oligonucleotides were tested against an RNA target, only the hexamer was necessary for hybridization (Le Tinévez et al., 1998). However, the aptamers led to such extensive cleavage by RNase H that the cleavage was non-specific for phosphodiester oligonucleotides in WGE. Specific antisense inhibition by these structures was seen with 2′-*O*-methyloligoribonucleotides, which act through an RNase H independent mechanism (Le Tinévez et al., 1998).

1.2.2. Tethered oligonucleotide probes

Another approach where binding to structured RNA rather than to the primary sequence is involved is the use of tethered oligonucleotide probes (TOPs) (Cload and Schepartz, 1994). These sequences recognize two short non-contiguous sequences that are proximal in the folded RNA. A random TOP library was used to identify single-stranded regions proximal to one another and able to bind short oligonucleotides. The TOPs consisted of a defined 8-mer sequence joined with a tether to a random 7-mer sequence. In order to determine the locations of the second binding sites when the TOPs were hybridized with the target RNA, an RNase H cleavage assay was used. It was found that the TOPs bind better to the target RNA than single-site probes.

1.3. Foldback triplex-forming oligonucleotides

Foldback triplex-forming oligonucleotides (FTFOs) contain a Watson–Crick domain, designed to bind to the complementary target sequence in the mRNA, and a Hoogsteen domain that folds back on the already formed double helix forming a triple helix through Hoogsteen hydrogen bonding (Kandimalla and Agrawal, 1994). The domains are joined covalently by an oligonucleotide loop or a synthetic linker. FTFOs were found to have a higher affinity for the target than conventional antisense and antigene oligonucleotides indicated by a higher melting temperature of these triplexes compared to ordinary duplexes or triplexes formed by three individual nucleotide strands (Kandimalla and Agrawal, 1994). In the same study it was found that FTFOs exhibit higher sequence specificity than conventional antisense oligonucleotides as the triplex formation is more sensitive to mismatches due to the double recognition of the target sequence (Kandimalla and Agrawal, 1994). The use of FTFOs as antisense inhibitors should therefore lead to less non-specific binding.

1.4. Selection of sequences with minimized non-specific binding

Computer programs can be used to select antisense oligonucleotide sequences based on the sequence of the target gene or mRNA. The program OligoProbeDesignStation extracts all possible sequences from a target gene or mRNA sequence (Mitsuhashi et al., 1994). The melting temperature (T_m) is calculated and homology is analyzed using GenBank to find cross-hybridizing genes. This could lead to design of antisense oligonucleotide sequences with higher selectivity.

With the computer program Oligomer, the genomic frequency of di-, tri- and hexamers contained within a given target sequence was determined (Han et al., 1994). It was found that hexamers are non-randomly distributed within the genome. Therefore, selecting antisense oligonucleotide sequences against less frequent hexamers could decrease the non-specific binding.

1.5. Empirically found targets

In a retrospective literature survey (Tu et al., 1998) it was found that the GGGA motif was present in targets for 47.6% of the antisense oligonucleotide sequences that (1) were shown to be the most effective in studies where at least 10 sequences were tested, or (2) were included in clinical trials. It was hypothesized (Tu et al., 1998) that the GGGA motif is a preferred target for RNase H as purine-rich RNA sections of DNA–RNA duplexes are preferred substrates for RNase H. Keeping this observation in mind, it would perhaps be favorable to select oligonucleotide sequences targeting this motif.

2. Conclusion

As described here, a variety of methods can be included in the search for optimal antisense oligonucleotide sequences. Many of the techniques are able to provide qualified candidates for antisense oligonucleotide effects. The future will probably bring even more, especially methods based on combinatorial screening. At this point, a combination of RNase H mapping of accessible sites and the use of combinatorial arrays seems like a good choice. If working with smaller transcripts, secondary structure analysis by programs such as Mfold should be valuable in cases where the suboptimal structures look similar. It is also of importance to consider non-specific effects of oligonucleotides by analyzing the homology with other genes or the full genome.

Acknowledgements

This work was supported financially, in part, by the Center for Drug Design and Transport and PharmaBiotec Research Center.

References

Akhtar, S., 1998. Antisense technology: selection and delivery of optimally acting antisense oligonucleotides. J. Drug Targeting 5, 225–234.

Bruice, T.W., Lima, W.F., 1997. Control of complexity constraints on combinatorial screening for preferred oligonucleotide hybridization sites on structured RNA. Biochemistry 36, 5004–5019.

Cload, S.T., Schepartz, A., 1994. Selection of structure-specific inhibitors of the HIV Rev–Rev response element complex. J. Am. Chem. Soc. 116, 437–442.

Crooke, S.T., 1995a. Molecular mechanism of action of oligonucleotides designed to interact with nucleic acids. In: Crooke, S.T. (Ed.), Therapeutic Applications of Oligonucleotides. R.G. Landes, Austin, pp. 11–38.

Crooke, S.T., 1995b. The selection of optimal RNA receptor sites for antisense effects. In: Crooke, S.T. (Ed.), Therapeutic Applications of Oligonucleotides. R.G. Landes, Austin, pp. 39–52.

Han, J., Zhu, Z., Hsu, C., Finley, W.H., 1994. Selection of antisense oligonucleotides on the basis of genomic frequency of the target sequence. Antisense Res. Dev. 4, 53–65.

Ho, S.P., Britton, D.H., Stone, B.A., Behrens, D.L., Leffet, L.M., Hobbs, F.W., Miller, J.A., Trainor, G.L., 1996. Potent antisense oligonucleotides to the human multidrug resistance-1 mRNA are rationally selected by mapping RNA-accessible sites with oligonucleotide libraries. Nucleic Acids Res. 24, 1901–1907.

Ho, S.P., Bao, Y.J., Lesher, T., Malhotra, R., Ma, L.Y., Fluharty, S.J., Sakai, R.R., 1998. Mapping of RNA accessible sites for antisense experiments with oligonucleotide libraries. Nat. Biotechnol. 16, 59–63.

Jaroszewski, J.W., 1998. Antisense drugs. In: Frøkjær, S., Christrup, L., Krogsgaard-Larsen, P. (Eds.), Peptide and Protein Drug Delivery. Alfred Benzon Symposium, Vol. 43. Munksgaard, Copenhagen, pp. 452–458.

Jaroszewski, J.W., Syi, J.L., Ghosh, M., Ghosh, K., Cohen, J.S., 1993. Targeting of antisense DNA: comparison of activity of anti-rabbit

β-globin oligodeoxyribonucleoside phosphorothioates with computer predictions of mRNA folding. Antisense Res. Dev. 3, 339–348.

Kandimalla, E.R., Agrawal, S., 1994. Single-strand-targeted triplex formation: stability, specificity and RNase H activation properties. Gene 149, 115–121.

Le Novère, 2000. Melting4, http://www.pasteur.fr/unites/neubiomol/meltinghome.html.

Le Tinévez, R., Mishra, R.K., Toulmé, J.J., 1998. Selective inhibition of cell-free translation by oligonucleotides targeted to a mRNA hairpin structure. Nucleic Acids Res. 26, 2273–2278.

Lima, W.F., Monia, B.P., Ecker, D.J., Freier, S.M., 1992. Implication of RNA structure on antisense oligonucleotide hybridization kinetics. Biochemistry 31, 12055–12061.

Lima, W.F., Brown Driver, V., Fox, M., Hanecak, R., Bruice, T.W., 1997. Combinatorial screening and rational optimization for hybridization to folded hepatitis C virus RNA of oligonucleotides with biological antisense activity. J. Biol. Chem. 272, 626–638.

Mathews, D.H., Sabina, J., Zuker, M., Turner, D.H., 1999. Expanded sequence dependence of thermodynamic parameters improves prediction of RNA secondary structure. J. Mol. Biol. 288, 911–940.

Matveeva, O., Felden, B., Audlin, S., Gesteland, R.F., Atkins, J.F., 1997. A rapid in vitro method for obtaining RNA accessibility patterns for complementary DNA probes: correlation with an intracellular pattern and known RNA structures. Nucleic Acids Res. 25, 5010–5016.

Milner, N., Mir, K.U., Southern, E.M., 1997. Selecting effective antisense reagents on combinatorial oligonucleotide arrays. Nat. Biotechnol. 15, 537–541.

Mishra, R.K., Toulmé, J.J., 1994. In vitro selection of antisense oligonucleotides targeted to a hairpin structure. CR Acad. Sci. III 317, 977–982.

Mishra, R.K., Le Tinevez, R., Toulmé, J.J., 1996. Targeting nucleic acid secondary structures by antisense oligonucleotides designed through in vitro selection. Proc. Natl. Acad. Sci. USA 93, 10679–10684.

Mitsuhashi, M., Cooper, A., Ogura, M., Shinagawa, T., Yano, K., Hosokawa, T., 1994. Oligonucleotide probe design — a new approach. Nature 367, 759–761.

Monia, B.P., Johnston, J.F., Geiger, T., Muller, M., Fabbro, D., 1996. Antitumor activity of a phosphorothioate antisense oligodeoxynucleotide targeted against C-raf kinase. Nat. Med. 2, 668–675.

Patzel, V., Sczakiel, G., 1998. Theoretical design of antisense RNA structures substantially improves annealing kinetics and efficacy in human cells. Nat. Biotechnol. 16, 64–68.

Patzel, V., Putlitz, J.Z., Wieland, S., Blum, H.E., Sczakiel, G., 1997. Theoretical and experimental selection parameters for HBV-directed antisense RNA are related to increased RNA–RNA annealing. Biol. Chem. 378, 539–543.

Pavlakis, G.N., Lockard, R.E., Vamvakopoulos, N., Rieser, L., RajBhandary, U.L., Vournakis, J.N., 1980. Secondary structure of mouse and rabbit a- and b-globin mRNAs: differential accessibility of α and β initiator AUG codons towards nucleases. Cell 19, 91–102.

Sczakiel, G., Homann, M., Rittner, K., 1993. Computer-aided search for effective antisense RNA target sequences of the human immunodeficiency virus type 1. Antisense Res. Dev. 3, 45–52.

Sohail, M., Akhtar, S., Southern, E.M., 1999. The folding of large RNAs studied by hybridization to arrays of complementary oligonucleotides. RNA 5, 646–655.

Southern, E.M., Case Green, S.C., Elder, J.K., Johnson, M., Mir, K.U., Wang, L., Williams, J.C., 1994. Arrays of complementary oligonucleotides for analysing the hybridisation behaviour of nucleic acids. Nucleic Acids Res. 22, 1368–1373.

Tu, G.C., Cao, Q.N., Zhou, F., Israel, Y., 1998. Tetranucleotide GGGA motif in primary RNA transcripts. Novel target site for antisense design. J. Biol. Chem. 273, 25125–25131.

Uhlmann, E., Peyman, A., 1990. Antisense oligonucleotides: a new principle. Chem. Rev. 90, 543–584.

Zuker, M., Jacobson, A.B., 1995. 'Well-determined' regions in RNA secondary structure prediction: analysis of small subunit ribosomal RNA. Nucleic Acids Res. 23, 2791–2798.

Zuker, M., Mathews, D.H., Turner, D.H., 1999. Algorithms and thermodynamics for RNA secondary structure prediction: a practical guide. In: Barciszewski, J., Clark, B.F.C. (Eds.), RNA Biochemistry and Biotechnology. Kluwer Academic, Dordrecht.

Antisense Oligodeoxynucleotide Inhibition of Vascular Angiotensin-Converting Enzyme Expression Attenuates Neointimal Formation

Evidence for Tissue Angiotensin-Converting Enzyme Function

Ryuichi Morishita, Gary H. Gibbons, Naruya Tomita, Lunan Zhang, Yasufumi Kaneda, Toshio Ogihara, Victor J. Dzau

Abstract—It has been proposed that vascular angiotensin-converting enzyme (ACE) plays an important role in regulating vascular growth. Indeed, ACE inhibitors have been reported to prevent neointimal formation after vascular injury in a rat carotid artery model. However, classic pharmacological experiments cannot exclude the potential contributions of hemodynamics and the circulating renin-angiotensin system (RAS). In this study, we used antisense oligodeoxynucleotide (ODN) to obtain local blockade of vascular ACE expression without effects on systemic hemodynamics and circulating RAS. To increase the effectiveness of antisense action, we modified the hemagglutinating virus of Japan–liposome ODN delivery method by cotransfection with nuclear protein (high mobility group 1 [HMG-1]) and RNase H. In vitro experiments showed the enhanced efficacy of antisense ODN by cotransfection of HMG-1 and RNase H compared with ODN alone. In vivo transfection of antisense ACE ODNs into intact uninjured rat carotid artery resulted in a significant reduction of vascular ACE activity, and cotransfection of HMG-1 and RNase H showed further reduction. We examined the effects of local blockade of vascular ACE expression on neointimal formation after vascular injury. Transfection of antisense ACE ODNs resulted in the attenuation of neointimal formation, whereas sense and scrambled ODNs did not. Blood pressure, heart rate, and serum ACE activity were not affected by antisense treatment. The magnitude of vascular ACE inhibition correlated with the suppression of the neointimal size. Overall, this study demonstrates that local antisense ODN inhibition of vascular ACE expression attenuates neointimal formation independent of hemodynamics and circulating RAS. The results support the existence of a functional tissue angiotensin system in the rat vessel wall. (*Arterioscler Thromb Vasc Biol.* 2000;20:915-922.)

Key Words: gene therapy ■ restenosis ■ renin-angiotensin system ■ antisense oligonucleotides ■ hemagglutinating virus of Japan

One of the current controversies in cardiovascular research is the existence of a functional tissue angiotensin system[1-4] in the blood vessel. The presence of a vascular angiotensin system has been reported previously.[5-7] Furthermore, we have described that vascular angiotensin-converting enzyme (ACE) expression is induced in the intimal smooth muscle cells of rat carotid artery and abdominal aorta in response to vascular injury.[8,9] This injury model has provided us with the opportunity to examine the functional role of local angiotensin production. Using a dose range of an ACE inhibitor, we demonstrated that the magnitude of neointimal lesion reduction correlated closely with the degree of vascular ACE inhibition.[10] We have interpreted these data as supportive evidence for a functional role of tissue angiotensin. However, the blockade of tissue angiotensin required an extremely high dosage of ACE inhibitors, which was invariably accompanied by the suppression of circulating renin angiotensin and the reduction of systemic blood pressure. Therefore, it is still unclear whether the local blockade of vascular angiotensin can indeed prevent neointimal formation without producing a systemic blockade of circulating renin angiotensin and/or without affecting hemodynamics. Furthermore, ACE inhibition also results in bradykinin accumulation and nitric oxide induction, which may contribute to the inhibition of neointimal hyperplasia.

Recent advances in molecular biology have provided us with the opportunity to study the function of a specific local gene product, such as vascular ACE. Using in vivo gene transfer, we have demonstrated that the overexpression of ACE locally in the uninjured rat carotid artery results in the development of vascular hypertrophy that occurs without an effect on blood pressure.[11] In the present report, we used a

Received August 6, 199; revision accepted October 26, 1999.

From the Division of Gene Therapy Science (R.M., Y.K.) and the Department of Geriatric Medicine (R.M., N.T., T.O.), Osaka University Medical School, Suita, Japan, and the Department of Medicine (G.H.G., L.Z., V.J.D.), Harvard Medical School, Brigham and Women's Hospital, Boston, Mass.

Correspondence to Ryuichi Morishita, MD, PhD, Associate Professor, Division of Gene Therapy Science, Osaka University Medical School, 2-2 Yamada-oka, Suita 565, Japan. E-mail morishit@geriat.med.osaka-u.ac.jp

Arterioscler Thromb Vasc Biol. is available at http://www.atvbaha.org

loss of function approach by using antisense oligodeoxynucleotides (ODNs) to ACE mRNA to examine the function of tissue ACE in the injured rat carotid artery in vivo. In the present study, we used a viral protein-liposome–mediated ODN transfer technique that made use of the liposome and the protein coat of the inactivated Sendai virus (hemagglutinating virus of Japan [HVJ]).[12,13] HVJ contains 2 envelope proteins, hemagglutinin-neuraminidase and fusion proteins, which mediate cell attachment and membrane fusion sequentially.[14,15] In the present study, we reasoned that if tissue ACE contributes to neointimal formation, we would observe a reduction of lesion formation by antisense ODNs in the absence of any effects on systemic blood pressure or the circulating renin-angiotensin system.

Methods

Oligonucleotides

Phosphorothioate ODNs were synthesized and purified by chromatography on NAP 10 columns (Pharmacia). The sequence of each ODN was as follows: antisense ACE 5′-GCCCCC*ATG*GCGCGGT-3′, position −8 to +8 of the rat sequence; sense ACE 5′-ACCGCGCC*ATG*GGGG*C*-3′. Scrambled ODN (5′-CCGTCGGTACCGGCCG-3′) was also used as a negative control. Synthetic ODNs were washed by 70% ethanol, dried, and dissolved in sterile Tris-EDTA buffer (10 mmol/L Tris and 1 mmol/L EDTA). The supernatant was purified over a NAP 10 column (Pharmacia) and quantified by spectrophotometry.[16,17]

Cell Culture

Neonatal vascular smooth muscle cells (VSMCs) were maintained in Waymouth media with 5% calf serum (CS), which had previously been inactivated first at 60°C for 1 hour and then at 58°C for another hour. (This protocol of heat inactivation abolishes serum ACE activity.[18,19]) Cells (1×10^6) were seeded onto 6-well plates and grown to 60% confluence. Previous data have shown that the addition of the nonhistone nuclear protein (high mobility group 1 [HMG-1]) enhances plasmid DNA uptake into the nucleus[20,21] and that RNase H enhances the antisense effect by degrading antisense-mRNA duplexes.[22,23] Accordingly, in the present study, phosphorothioate ODN was incubated with or without HMG-1 (200 μg ODN and 64 μg HMG-1) plus RNase H (6 U in liposomes) at 20°C for 1 hour. This complex was then encapsulated in HVJ-liposome. HVJ-liposome (500 μL) containing 3 μmol/L of encapsulated ODN was then added to the wells and incubated for 5 minutes at 4°C and 30 minutes at 37°C. After transfection, fresh medium containing 5% CS was added, and the cells were incubated in a CO_2 incubator. On day 3 or 5 after transfection, cells were homogenized, and ACE activity was measured. The enzymatic activity, expressed as hippuryl-L-histidyl-L-leucine–hydrolyzing activity per milligram of homogenate protein, was determined by the modified method of Cushman and Cheung.[24] The specificity of the ACE activity was confirmed by complete inhibition by either quinaprilat or neutralizing antibodies to ACE.[18,19]

HVJ-Liposome Preparation

Briefly, phosphatidylserine, phosphatidylcholine, and cholesterol were mixed in a weight ratio of 1:4.8:2 to create a lipid mixture. Dried lipid was hydrated in a balanced salt solution containing ODN. Liposomes were prepared by shaking and sonication. Purified HVJ (Z strain) was inactivated by UV irradiation (110 erg · mm^{-2} · s^{-1}) for 3 minutes just before use. The liposome suspension (0.5 mL) was mixed with HVJ (10 000 hemagglutinating units) in a total volume of 4 mL of balanced salt solution. The mixture was incubated at 4°C for 5 minutes and for 30 minutes with shaking at 37°C. Free HVJ was removed from the HVJ-liposome by sucrose density gradient centrifugation. The top layer of sucrose gradient was collected for use.[16–19]

Cotransfection of HMG-1 and Antisense ACE ODNs

Phosphorothioate ODN was incubated with or without HMG-1 (200 μg ODN and 64 μg HMG-1) at 20°C for 1 hour. Then, 500 μL of HVJ-liposome (3 μmol/L of encapsulated ODN in liposomes) was added to the wells and incubated for 5 minutes at 4°C and 30 minutes at 37°C. After transfection, fresh medium containing 5% CS was added, and the cells were incubated in a CO_2 incubator. On day 3 or 5 after transfection, cell ACE activity was measured.

Cotransfection of RNase H and Antisense ACE ODNs

Before liposome preparation, purified RNase H (GIBCO) and/or DNA-RNA hybrids were combined with antisense ACE ODN. The following procedure was described above. DNA-RNA hybrids were made by the annealing of poly A(RNA)–poly T(DNA) by polymerase chain reaction. DNA-DNA [poly A(DNA)–poly T(DNA)] hybrids were used as negative controls. Briefly, equal amounts of poly A and poly T were mixed. Then this solution was heated to 80°C for 5 minutes and gradually decreased to room temperature for making a double strand. HVJ-liposome (500 μL, 3 μmol/L of encapsulated ODN in liposomes) was added to the wells and incubated for 5 minutes at 4°C and 30 minutes at 37°C. After transfection, fresh medium containing 5% CS was added, and the cells were incubated in a CO_2 incubator. On day 3 after transfection, cell ACE activity was measured.

In Vivo Transfer Into Intact Rat Carotid Artery

Male Sprague-Dawley rats (400 to 500 g, Charles River Breeding Laboratories, Atsugi, Kanagawa, Japan) were anesthetized with ketamine, and the left common carotid artery was surgically exposed.[11,17,18] A cannula was introduced into the common carotid via the external carotid artery. HVJ-liposome complex (200 μL, 10 μmol/L ODN with or without HMG-1 and RNase H [6 U in liposomes]) was infused into the segment and incubated for 10 minutes at room temperature. After a 10-minute incubation, the infusion cannula was removed. After the transfection, blood flow to the common carotid was restored by release of the ligatures, and the wound was then closed. For the measurement of vascular ACE activity, rats were euthanized at 7 days after transfection. After infusion of PBS, carotid arteries were removed and dissected free of periadventitial tissues and immediately frozen in liquid nitrogen. On the day of assay, the vessels were thawed, weighed, and homogenized in 50 mmol/L KPO_4 (pH 7.5). ACE activity was determined as described above.[24] Vascular ACE level was expressed as enzymatic activity per milligram of protein.

In Vivo Transfection of Antisense ODNs Into Rat Injured Carotid Artery

In vivo gene transfer was performed under the following conditions: vascular injury of the common carotid was produced by the passage and inflation of a balloon catheter (a 2F Fogarty catheter) through an arteriotomy in the external carotid artery 3 times.[16,17] The injured segment was transiently isolated by temporary ligatures. HVJ-liposome complex (200 μL) containing antisense ACE ODN, sense ACE ODN (each at 10 μmol/L with or without 6 U RNase H and HMG-1 contained in liposomes), or scrambled ODN (10 μmol/L) with HMG-1 and RNase H was incubated within the lumen for 10 minutes. Two weeks after injury and transfection, each carotid artery was processed for ACE activity and morphological study. For histological analyses, a segment of each artery was perfusion-fixed with 4% paraformaldehyde and subsequently processed. Medial and luminal areas were measured on a digitizing tablet (model 2200, South Micro Instruments) after staining with hematoxylin.[16,17] The medial area was readily demarcated as the vessel area between the internal and external elastic laminae. At least 3 individual sections from the middle of the transfected arterial segments were analyzed. Animals were coded so that the analysis was performed without the knowledge of which treatment each individual animal received.

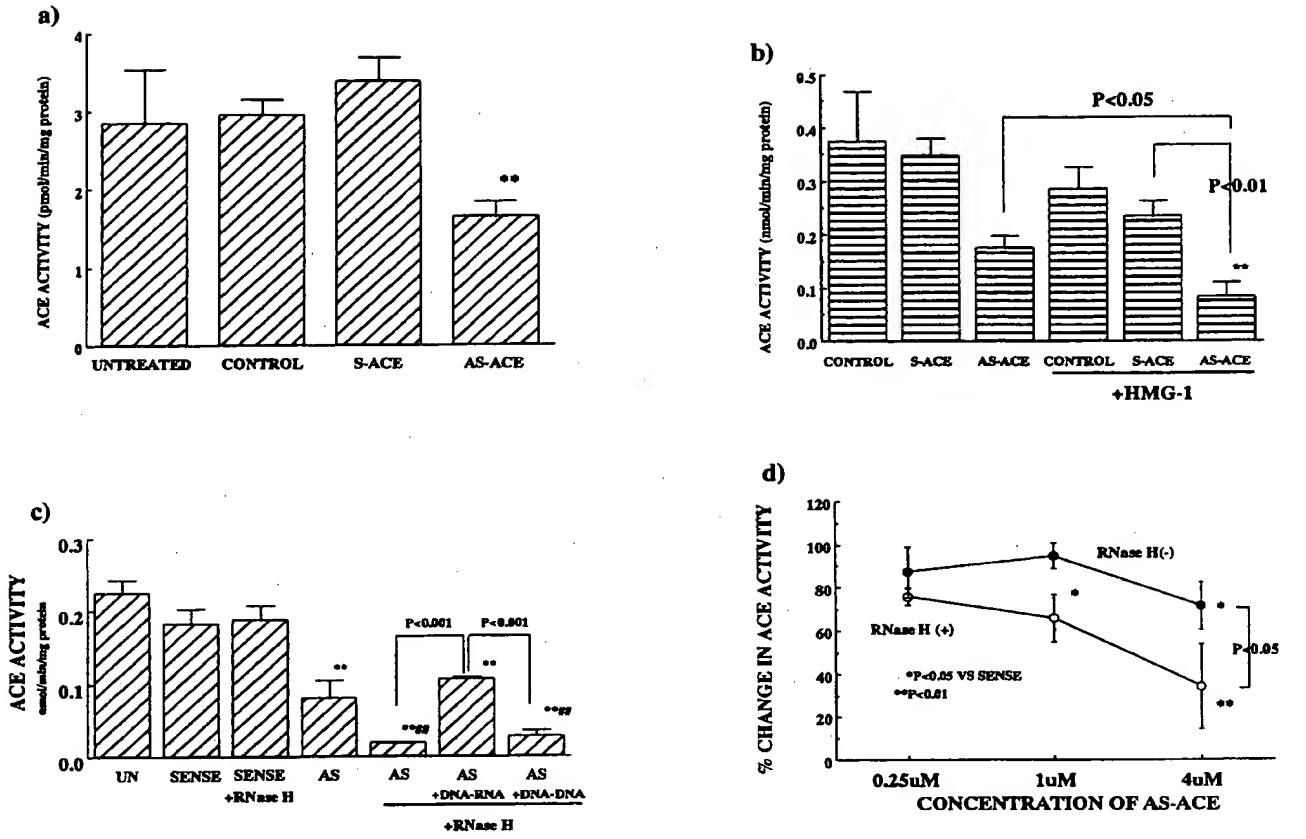

Figure 1. Effect of in vitro transfection of antisense ACE ODN on ACE activity. a, Effect of transfection of antisense ACE ODNs on ACE activity at 5 days after transfection by HVJ-liposome method. Untreated indicates untreated VSMCs; control, VSMCs treated with HVJ-liposome complex without ODNs; S-ACE, VSMCs treated with sense ODNs in HVJ-liposome complex; and AS-ACE, VSMCs treated with antisense ODNs in HVJ-liposome complex. $^{**}P<0.01$ vs untreated. b, Effect of cotransfection of HMG-1 and antisense ACE ODNs on ACE activity at 5 days after transfection. Control indicates untreated VSMCs; S-ACE, sense ODN–treated VSMCs; and AS-ACE, antisense ODN–treated VSMCs. $^{**}P<0.01$ vs untreated VSMCs. c, Effect of in vitro cotransfection of RNase H and antisense ACE ODNs (3 μmol/L) on ACE activity. UN indicates untreated VSMC; SENSE, VSMCs transfected with sense ODNs; sense+RNase H, VSMCs cotransfected with sense ODNs and RNase H (6 U); AS, VSMCs transfected with antisense ODNs; AS+RNase H, VSMCs cotransfected with antisense ODNs and RNase H (6 U); AS+DNA-RNA+RNase H, VSMCs cotransfected with antisense ODNs, RNase H, and DNA-RNA hybrid; and AS+DNA-DNA+RNase H, VSMCs cotransfected with antisense ODNs, RNase H, and DNA-DNA hybrid. $^{**}P<0.01$ vs respective VSMCs transfected with sense ODNs; $\#\#P<0.01$ vs respective VSMCs transfected with antisense ODN. d, Dose effect of antisense ACE ODNs coupled with HMG-1 with or without RNase H (6 U) on ACE activity. ○ indicates antisense ACE ODNs coupled with HMG-1 but without RNase H; ●, antisense ACE ODNs with HMG-1 and RNase H. $^{*}P<0.05$ and $^{**}P<0.01$ vs sense ACE ODNs (with or without RNase H, respectively).

Miscellaneous Measurements

Blood pressure was measured by direct measurement with use of a catheter inserted into the femoral artery of a conscious animal after recovery from anesthesia (48 hours after anesthesia). Serum ACE activity was measured from blood obtained at this time by use of the assay of Cushman and Cheung,[24] as described earlier in this article.

Statistical Analysis

All values are expressed as mean±SEM. ANOVA with a subsequent Bonferroni test was used to determine significant differences in multiple comparisons. A value of $P<0.05$ was considered significant.

Results

Modification of Antisense ODNs by HVJ-Liposome Method

Using the HVJ-liposome method, we first performed in vitro transfection of antisense ACE ODNs into neonatal VSMCs, which are known to express high levels of ACE.[26] A significant reduction in cellular ACE activity was observed at 5 days after transfection with antisense ACE phosphorothioate ODN (3 μmol/L in liposomes, Figure 1a). Next, we examined the effect of cotransfection of the nonhistone nuclear protein HMG-1 and the antisense ACE phosphorothioate ODN into cultured neonatal VSMCs. HMG-1 has been reported to bind DNA and transport it into the nuclei,[20,27–29] thereby increasing the gene expression of the transfected plasmid.[20] In the present study, we reasoned that cotransfection of ODN with HMG-1 contained in HVJ-liposome might enhance the nuclear uptake and prolong the action of ODN. As shown in Figure 1b, an increased inhibitory effect resulting from the cotransfection of HMG-1 and antisense ODN was observed, because a measured decrease in ACE activity could be seen at 5 days after transfection with HVJ-liposome. In contrast, HMG-1 alone did not affect ACE activity. We also studied the enhanced effect of HMG-1 on a dose range of antisense ODN. Our

results demonstrate that the cotransfection of antisense ODN with HMG-1 in HVJ-liposome was consistently better than antisense ODN without HMG-1 (data not shown).

Within the nucleus, antisense ODN hybridizes with the target mRNA, and the resultant hybrid is degraded by RNase H as 1 of the major mechanisms of antisense ODN action.[30–32] In mammalian cells, RNase H activity is rather low compared with activity in the frog oocyte,[22,23,33] and one may expect that the contribution of RNase H to antisense ODN action to be limited. However, numerous recent reports have shown significant decreases in transcript levels of the targeted genes with antisense ODN treatment.[16,17,34] Indeed, our results showed a reduction of ACE mRNA expression (data not shown). Therefore, we examined whether the cotransfection of purified RNase H with antisense ACE ODN would result in an enhanced inhibition of ACE expression. We observed that cotransfection of RNase H and antisense phosphorothioate ODN resulted in a significant decrease in ACE activity compared with antisense phosphorothioate ODN alone at 5 days after transfection into VSMCs in vitro (Figure 1c). This increased efficacy was due to the transfection of additional exogenous RNase H into VSMCs, because we cotransfected synthetic poly A(RNA)–poly T(DNA) hybrids (DNA-RNA hybrids), which have been used previously to test the RNase H activity in a cell-free system,[22] but not DNA–DNA ligand. There was an attenuated decrease in ACE activity produced by antisense ACE-ODN treatment (Figure 1d). Reduction of ACE mRNA was also enhanced by cotransfection of RNase H and antisense ACE ODN (data not shown). To exclude the nonspecific effect of RNase H, cotransfection of RNase H and methylphosphonate antisense ODN was also performed, because RNase H can cleave RNA-DNA hybrids of unmodified or phosphorothioate ODN but not those of methylphosphonate ODN.[22,23] As expected, the increase in the in vitro inhibitory effect of phosphorothioate antisense ODN by cotransfection of RNase H and HMG-1 was not observed when methylphosphonate ODNs were used (antisense ACE without RNase H, 55.2±6.0%; antisense ACE with RNase H, 76.1±9.8%; $P>0.05$). A 6 μmol/L concentration enwrapped in liposomes was used. Values are expressed as percentage inhibition of ACE activity of representative sense ACE methylphosphonate ODN–treated VSMCs. Finally, we postulated that the mechanisms of enhanced effects of HMG-1 and RNase H are synergistic. Accordingly, we examined the inhibitory effect of cotransfection of RNase H and antisense ACE ODN coupled with HMG-1. As shown in Figure 1d, cotransfection of antisense phosphorothioate ODN with HMG-1 and RNase H resulted in a further significant decrease in ACE activity 5 days after treatment compared with the transfection of antisense phosphorothioate ODN coupled with HMG-1 without RNase H. Cotransfection of RNase H and HMG-1 did not result in any cytotoxic effect as assessed by microscopic examination.

In Vivo Transfection of Antisense ACE ODNs Into Rat Intact Vessels

By use of this technology, the enhanced effect of antisense ACE ODNs by cotransfection of HMG-1 and RNase H was also investigated in vivo in the intact rat carotid artery. One week after transfection, vascular ACE activity was measured. Antisense phosphorothioate ACE ODNs significantly decreased ACE activity compared with sense ODNs (Figure 2). Cotransfection of HMG-1, RNase H, and antisense ACE ODN decreased ACE activity further compared with antisense ACE ODN without HMG-1 and RNase H. There was no significant difference in ACE activity in the intact, sense ODN–treated vessels compared with the activity in vessels treated with sense ODN with HMG-1 and RNase H. No morphometric differences were observed between antisense versus sense ODN–treated uninjured vessels (data not shown).

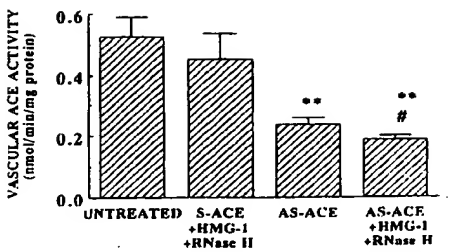

Figure 2. Inhibitory effect of antisense ACE ODNs on vascular ACE activity in intact uninjured carotid arteries with or without RNase H and HMG-1 in vivo. Untreated indicates sham-operated vessels (n=7); S-ACE+HMG-1+RNase H, vessels treated with sense ODNs with HMG-1 and RNase H (n=8); AS-ACE, vessels treated with antisense ODNs without HMG-1 and RNase H (n=8); and AS-ACE+HMG-1+RNase H, vessels treated with antisense ODNs with HMG-1 and RNase H (n=9). $^{**}P<0.01$ vs untreated; $\#P<0.05$ vs AS-ACE.

Effect of Antisense ACE ODNs on Neointimal Formation

We also examined the effect of antisense ACE ODN on the neointimal formation after balloon injury. Administration of antisense ODN with HMG-1 and RNase H in HVJ-liposome significantly decreased vascular ACE activity at 2 weeks after transfection (scrambled ODN, 19.4±2.3 pmol · min^{-1} · mg $protein^{-1}$; antisense ODN, 5.6±1.8 pmol · min^{-1} · mg $protein^{-1}$; $P<0.01$). The inhibitory effect of antisense ODNs with HMG-1 and RNase H was not accompanied by the inhibition of serum ACE activity (Table 1). In contrast, the other treatment groups failed to show any reduction in vascular ACE. Moreover, administration of antisense ACE ODNs (10 μmol/L) cotransfected with HMG-1 and RNase H (6 U) resulted in the inhibition of neointimal formation by 50% (Figures 3a and 3b). Similarly, neointimal areas were also reduced by antisense ACE ODN treatment accompanied with the reduction of vascular ACE activity, whereas no significant changes in medial areas were observed in any

TABLE 1. Effects of Transfection of Antisense ACE ODNs on Serum ACE Activity, Blood Pressure, and Heart Rate

	Serum ACE Activity, nmol · min^{-1} · h^{-1}	Blood Pressure, mm Hg	Heart Rate, bpm
Sense ODN with HMG-1 and RNase H	2.15±0.27	127±3	432±25
Antisense ODN with HMG-1 and RNase H	2.60±0.65	122±4	428±31

Values are mean±SEM. There was no significant difference in serum ACE activity, blood pressure, and heart rate between rats transfected with sense ACE ODN and rats transfected with antisense ACE ODN.

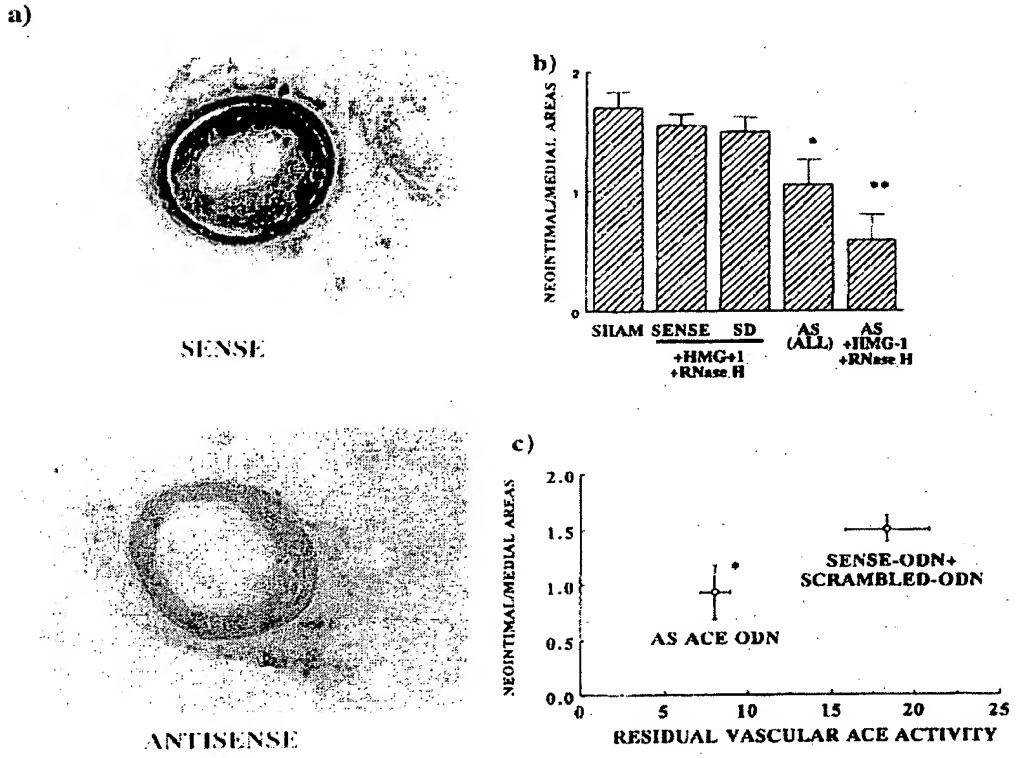

Figure 3. a, Effect of antisense ACE ODNs on neointimal formation. Representative cross sections are as follows: sense, injured carotid artery transfected with sense ACE ODN; antisense, injured carotid artery transfected with antisense ACE ODN in combination with HMG-1 and RNase H. Magnification ×40. b, Inhibitory effect of antisense ACE ODNs on neointimal formation after vascular injury in vivo. Sense indicates vessels treated with sense ODN with HMG-1 and RNase H (n=3); SD, vessels treated with scrambled ODN with HMG-1 and RNase H (n=6); AS (all), all vessels treated with antisense ODN (n=10); and AS+HMG-1+RNase H, vessels treated with antisense ODN with HMG-1 and RNase H (n=5). *$P<0.05$ and **$P<0.01$ vs sense or SD. c, Correlation of residual vascular ACE activity and neointimal size. Sense-ODN+scrambled-ODN indicates vessels treated with sense ODN (n=3) and scrambled ODN (n=6) with HMG-1 and RNase H; AS ACE ODN, vessels treated with antisense ODN with (n=5) and without HMG-1 and RNase H (n=5). *$P<0.05$ vs sense-ODN+scrambled-ODN in vascular ACE activity.

group (Table 2). No effects on blood pressure or heart rate (Table 1) were observed. Residual vascular ACE activity in the lesion after treatment exhibited good correlation with the size of the remaining neointimal lesion, as shown in Figure 3c. Neither sense ODN nor scrambled ODN with HMG-1 and RNase H had any effect on the neointimal formation.

Discussion

Angiotensin II (Ang II), a potent vasoconstrictor, has been shown to possess growth-promoting activity. In vitro, Ang II stimulates vascular smooth muscle growth that is mediated by the induction of autocrine growth factors: platelet-derived growth factor, basic fibroblast growth factor, transforming growth factor-β, and insulin growth factor.[4,6] This function of Ang II in vivo has been suggested by studies using Ang II infusion, ACE inhibitors, and vascular injury.[10,35,36] However, the contribution of the direct growth effect of Ang II versus its hemodynamic effect to these in vivo actions cannot be dissected with these approaches. Furthermore, recent data suggest that Ang II is produced in local tissues in addition to

TABLE 2. Neointimal Areas, Medial Areas, and Residual Vascular ACE Activity in Vessels Transfected With Sense, Scrambled, and Antisense ODNs

	Neointimal Areas, mm^2	Medial Areas, mm^2	Residual Vascular ACE Activity, $nmol \cdot min^{-1} \cdot mg\ protein^{-1}$
Sham	0.238±0.026	0.140±0.001	ND
Sense	0.218±0.04	0.141±0.016	230±31
Scrambled	0.245±0.01	0.164±0.014	202±11
Antisense	0.157±0.029*	0.149±0.021	98±6†
Antisense+RNase H+HMG-1	0.095±0.028†	0.159±0.015	56±7†

Values are mean±SEM. ND indicates not determined.
*$P<0.05$ and †$P<0.01$ vs sense ODNs.

the circulating Ang II peptide hormone. This concept of a tissue angiotensin system proposes that a significant portion of the growth response in the vessel wall is due to local Ang II. Controversy exists as to the validity of this hypothesis, because inhibition of the local system without systemic effects has not been possible when the current pharmacological approach is used.

Local vascular injury is a good model for examining the effect of increased local tissue ACE. We have reported that 1 to 2 weeks after balloon angioplasty injury of the rat carotid artery or abdominal aorta, ACE expression is induced in the injured vessel, especially in the neointima.[9] The level of vascular ACE and, consequently, Ang II correlated with the size of the neointima.[10] To examine directly the importance of local ACE in regulating Ang II production and function, we have previously used in vitro and in vivo gene transfer of ACE into cultured VSMCs and intact vessels.[18,19] We have demonstrated that transfection of ACE cDNA into VSMCs in vitro results in a significant increase in ACE activity and in Ang II–mediated cellular hypertrophy.[18,19] Transfection of ACE cDNA into rat intact carotid artery results in a significant increase in vascular ACE accompanied by a local angiotensin-mediated hypertrophy.[11] Because the transfected segment is exposed to the same blood pressure and neurohormones (including circulating renin, ACE, and Ang II levels) as the control segment, these results are strong evidence for a local ACE effect in Ang II production and, consequently, function. Taken together, these data suggest that in addition to the circulating RAS, local angiotensin production is an important modulator of vascular structure.

In the present study, we examined the role of local blockade of the vascular angiotensin system in the prevention of VSMC accumulation after balloon injury by using antisense ODNs to block the local ACE expression without systemic effects. Hence, we addressed the following questions: (1) Does vascular ACE mediate vascular hyperplasia after balloon injury of the rat carotid artery? (2) Is the inhibition of neointimal formation by anti-renin angiotensin agents due to the blockade of local or circulating renin angiotensin or both? (3) Does local angiotensin have a specific role independent of circulating renin angiotensin and/or hemodynamics? These questions cannot be answered by the current pharmacological approach, because the effect of ACE inhibitors and Ang II receptor antagonists on neointimal formation is accompanied by a parallel inhibition of serum ACE activity and fall in blood pressure.[10,35,36]

To accomplish efficient transfection of antisense ODNs, we used the efficient HVJ-liposome method and modified it further by cotransfection of HMG-1 and RNase H. Antisense ODNs are known to be taken up via receptor-mediated endocytosis, leading to limitation by lower cellular uptake and degradation by endocytosis-lysosomal pathways.[30–32] Using FITC-labeled ODNs, we have reported that ODNs encapsulated in HVJ-liposomes can enter directly into the cytoplasm and immediately into the nucleus, resulting in much less dosage than direct transfer to achieve the same effect.[13,17,37] This approach takes advantage of the properties of HVJ, a *Paramyxovirus* that can fuse with cell membranes at neutral pH.[38] The viral proteins of the HVJ-liposome complex fuse with the cell surface membrane,[39,40] and the antisense ODN is consequently introduced directly into the cytoplasm. The character of the HVJ-liposome method, ie, membrane fusion, resulted in a marked increase in the efficiency of antisense ODNs compared with passive uptake. The accumulation of ODNs into nuclei after entering the cytoplasm has been reported to be due to passive diffusion,[41] because the existence of a nuclear binding site of ODNs is known.[42] Although the knowledge of a nuclear binding site of ODNs is relatively limited, it is logical to think that the number of binding sites may be a rate-limiting step for the entrance of ODNs into the nuclei, where RNase H is postulated to function as a major mechanism of the antisense ODN effect. Therefore, we thought that cotransfection of HMG-1 with antisense ODN might enhance the effect by increasing the amount of ODN that is anticipated to function with RNase H in the nuclei, because HMG-1 has been postulated to bind DNA and carry it into the nuclei by a different pathway, the ODN binding site.[20,21] As expected, our data showed that HMG-1 will also facilitate antisense ODN translocation into the VSMC nucleus because cotransfection of HMG-1 and antisense ACE ODNs in HVJ-liposome resulted in a significantly greater inhibition of cellular ACE activity compared with antisense ODN alone (Figure 1b). However, our present results cannot fully explain whether the enhancement of HMG-1 on antisense action is due to the enhanced nuclear translocation of antisense ODNs.

Accordingly, we reasoned that cotransfection of RNase H and ODNs can also increase the effectiveness of antisense ODNs in neonatal VSMCs. Because the HVJ-liposome method can also deliver protein besides plasmid DNA and ODN into cells, we added exogenous excess–purified RNase H to the preparation and demonstrated that their modification resulted in an enhanced effect of the antisense ODN. Introduction of additional exogenous RNase H may overcome the rate limitations of low endogenous RNase H concentrations. The specificity of exogenous RNase H action was supported by the demonstration that this effect was inhibited by cotransfection of the synthetic DNA-RNA hybrid but not the synthetic DNA-DNA hybrid (Figure 1c). Further evidence for the specificity of the effect of RNase H is also supported by the observation that cotransfection of RNase H and methylphosphonate ODNs had no enhanced effects because methylphosphonate ODNs are not substrates of RNase H. It has been reported that phosphorothioate ODN is a better target for RNase H than is unmodified ODN.[33] Given the widespread usage of phosphorothioate ODNs, this modification by RNase H may aid in the application of antisense phosphorothioate ODNs. Taken together, these results show that these modifications of antisense strategy are effective and that they overcome the 2 limitations to the success of the antisense technology, ie, high side effects and low efficiency. The present study demonstrates that using HMG-1 and RNase H combined with antisense phosphorothioate ODNs can markedly increase the effect and decrease the dose of antisense ODNs, although the exact mechanisms of the current modification of antisense delivery using HMG-1 and RNase H has not yet been clarified.

Using this improved and efficient delivery method, we examined the transfection of antisense ACE ODNs into balloon-injured rat carotid arteries. As previously described, a single transfection of ODN was sustained at least up to 2 weeks after transfection.[17,37] Transfection of

antisense ACE ODNs resulted in the attenuation of neointimal formation after vascular injury, whereas transfection of sense and scrambled ODNs did not. Importantly, these changes were not accompanied by any changes in hemodynamics (blood pressure and heart rates) or serum ACE. Our data provide evidence that local vascular ACE plays a role in VSMC accumulation in vivo in injured rat carotid arteries that is independent of hemodynamics (no change in blood pressure) and circulating renin angiotensin (no change in serum ACE activity). It is important to point out that although our data support an important functional role of the local angiotensin system, they do not preclude a contribution of the circulating renin-angiotensin system as well. Alternatively, an increase in locally produced bradykinin might affect neointimal hyperplasia, because ACE is also a rate-limiting step in the bradykinin pathway. Further studies are necessary to elucidate the role of bradykinin in this model. Because the present study was performed to examine the existence and function of the tissue angiotensin system in the rat carotid injury model, it was not designed to address the clinical relevance to human restenosis, which is a condition with complex pathophysiological processes beyond neointimal hyperplasia. Indeed, the results of MERCATOR[43] and MARCATOR[44] trials of ACE inhibition on human restenosis were negative. However, the problems of dosing and timing of therapy in these human studies preclude a definitive conclusion. Alternatively, the failure of those studies may be due to the presence of non-ACE pathways generating Ang II, because chymase, which generates Ang II, has been reported in humans.[45,46] Regardless of these issues, our data provide support for the concept that the production of angiotensin locally can result in altered tissue function and structure. Accordingly, one must view the local angiotensin system in the context of tissue function beyond blood pressure regulation. Finally, the present study demonstrated partial inhibition of neointimal formation, whereas the previous findings that made use of antisense ODNs against cell cycle regulatory genes showed almost complete inhibition.[16,17] This discrepancy may be due to the multicomplex of the process in the formation of restenosis. The clinical efficacy of antisense strategy against specific growth factors must be discussed in the future.

Acknowledgments

This study was partially supported by grants from the Japan Health Sciences Foundation, the Mochida Memorial Foundation for Medical and Pharmaceutical Research, the Hoan-sya Foundation, the Japan Cardiovascular Research Foundation, and the Japan Heart Foundation Research Grant; a Grant-in-Aid from the Tokyo Biochemical Research Foundation; and a Grant-in-Aid from the Ministry of Education, Science, Sports, and Culture.

References

1. Dzau VJ, Brody T, Ellison KE, Pratt RE, Ingelfinger JR. Tissue specific regulation of renin expression in the mouse. *Hypertension*. 1987; 9(suppl III):III-36–III-41.
2. Dzau VJ, Burt DW, Pratt RE. Molecular biology of the renin angiotensin system. *Am J Physiol*. 1988;255:F563–F573.
3. Campbell DJ, Habener JF. Angiotensinogen gene is expressed and differentially regulated in multiple tissues of the rat. *J Clin Invest*. 1986;78: 31–39.
4. Krieger JE, Dzau VJ. Molecular biology of hypertension. *Hypertension*. 1991;18(suppl I):I-3–I-17.
5. Morishita R, Higaki J, Miyazaki M, Ogihara T. Possible role of the vascular renin angiotensin system in hypertension and vascular hypertrophy. *Hypertension*. 1992;19(suppl II):II-62–II-67.
6. Dzau VJ, Gibbons GH, Pratt RE. Molecular mechanisms of vascular renin-angiotensin system in myointimal hyperplasia. *Hypertension*. 1991; 18(suppl II):II-100–II-105.
7. Morishita R, Higaki J, Okunishi H, Tanaka T, Ishii K, Nagano M, Mikami H, Ogihara T, Murakami K, Miyazaki M. Changes in gene expression of the renin-angiotensin system in two-kidney, one clip hypertensive rats. *J Hypertens*. 1991;9:187–192.
8. Rakugi H, Jacob HJ, Krieger JE, Ingelfinger JR, Pratt RE. Vascular injury induces angiotensinogen gene expression in the media and neointima. *Circulation*. 1993;87:283–290.
9. Rakugi H, Kim DK, Krieger JE, Wang DS, Dzau VJ, Pratt RE. Induction of angiotensin converting enzyme in the neointima after vascular injury: possible role in restenosis. *J Clin Invest*. 1994;93:339–346.
10. Rakugi H, Wang DS, Dzau VJ, Pratt RE. Potential importance of tissue angiotensin-converting enzyme inhibition in preventing neointima formation. *Circulation*. 1994;90:449–455.
11. Morishita R, Gibbons GH, Ellison KE, Lee WS, Zhang L, Yu H, Kaneda Y, Ogihara T, Dzau VJ. Evidence for direct local effect of angiotensin in vascular hypertrophy: in vivo gene transfer of angiotensin converting enzyme. *J Clin Invest*. 1994;94:978–984.
12. Kaneda Y, Uchida T, Makeda E, Nakanishi M, Okada Y. Entry of diphtheria toxin into cells: possible existence of cellular factor(s) for entry of diphtheria toxin into the cells was studied in somatic cell hybrids and hybrid toxins. *J Cell Biol*. 1984;98:466–472.
13. Morishita R, Gibbons GH, Kaneda Y, Ogihara T, Dzau VJ. Pharmacokinetics of antisense oligonucleotides (cyclin B1 and cdc 2 kinase) in the vessel wall: enhanced therapeutic utility for restenosis by HVJ-liposome method. *Gene*. 1994;149:13–19.
14. Okada Y. Factors in fusion of cells by HVJ. *Curr Top Microbiol Immunol*. 1969;48:102–128.
15. Homma M. Trypsin action on the growth of Sendai virus in tissue culture cells, I: restoration of the infectivity for L cells by direct action of trypsin on L cell-borne Sendai virus. *J Virol*. 1971;8:619–629.
16. Morishita R, Gibbons GH, Ellison KE, Nakajima M, Zhang L, Kaneda Y, Ogihara T, Dzau VJ. Single intraluminal delivery of antisense cdc 2 kinase and PCNA oligonucleotides results in chronic inhibition of neointimal hyperplasia. *Proc Natl Acad Sci U S A*. 1993;90:8474–8479.
17. Morishita R, Gibbons GH, Ellison KE, Nakajima N, von der Leyen H, Zhang L, Kaneda Y, Ogihara T, Dzau VJ. Intimal hyperplasia after vascular injury is inhibited by antisense cdk 2 kinase oligonucleotides. *J Clin Invest*. 1994;93:1458–1464.
18. Morishita R, Gibbons GH, Kaneda Y, Ogihara T, Dzau VJ. Novel and effective gene transfer technique for study of vascular renin angiotensin system. *J Clin Invest*. 1993;91:2580–2585.
19. Morishita R, Gibbons GH, Kaneda Y, Ogihara T, Dzau VJ. Novel in vitro gene transfer method for study of local modulators in vascular smooth muscle cells. *Hypertension*. 1993;21:894–899.
20. Kaneda Y, Iwai K, Uchida T. Increased expression of DNA cointroduced with nuclear protein in adult rat liver. *Science*. 1989;243:375–378.
21. Lilley DM. DNA-protein interactions. HMG has DNA wrapped up. *Nature*. 1992;357:282–283.
22. Walder RY, Walder JA. Role of RNase H in hybrid-arrested translation by antisense oligonucleotides. *Proc Natl Acad Sci U S A*. 1988;85: 5011–5015.
23. Busen W. Purification, subunit structure, and serological analysis of calf thymus ribonuclease H1. *J Biol Chem*. 1980;255:9434–9443.
24. Cushman DW, Cheung HS. Spectrophotometric assay and properties of the angiotensin-converting enzyme of rabbit lung. *Biochem Pharmacol*. 1970;20:11637–11648.
25. Deleted in proof.
26. Rakugi H, Wang D, Giachelli C, Schwartz SM, Dzau VJ, Pratt RE. Developmentally regulated production of angiotensin converting enzyme in cultured rat vascular smooth muscle cells. *J Hypertens*. 1992;10:S127. Abstract.
27. Hughes EN, Engelsberg BN, Billings PC. Purification of nuclear proteins that bind to cisplatin-damaged DNA: identity with high mobility group proteins 1 and 2. *J Biol Chem*. 1992;267:13520–13527.
28. PM Pil, Lippard SJ. Specific binding of chromosomal protein HMG1 to DNA damaged by the anticancer drug cisplatin. *Science*. 1992;256: 234–237.
29. Fisher RP, Lisowsky T, Parisi MA, Clayton DA. DNA wrapping and bending by a mitochondrial high mobility group-like transcriptional activator protein. *J Biol Chem*. 1992;267:3358–3367.
30. Marcus-Sekura CJ. Techniques for using antisense oligodeoxynucleotides to study gene expression. *Anal Biochem*. 1988;172:289–295.

31. Stein CA, Cohen JS. Oligodeoxynucleotides as inhibitors of gene expression: a review. *Cancer Res.* 1988;48:2659–2668.
32. Akhtar S, Juliano RL. Cellular uptake and intracellular fate of antisense oligonucleotides. *Trends Cell Biol.* 1992;2:139–144.
33. Agrawal S, Mayrand SH, Zamecnik PC, Pederson T. Site-specific excision from RNA by RNase H and mixed-phosphate-backbone oligodeoxynucleotides. *Proc Natl Acad Sci U S A.* 1990;87:1401–1405.
34. Simons M, Edelman ER, Dekeyser JL, Langer R, Rosenberg RD. Antisense c-myb oligonucleotides inhibit intimal arterial smooth muscle cell accumulation in vivo. *Nature.* 1992;359:67–70.
35. Kauffman RF, Bean JS, Zimmerman KM, Brown RF, Steinberg MI. Losartan, a nonpeptide angiotensin II (Ang II) receptor antagonist, inhibits neointima formation following balloon injury to rat carotid arteries. *Life Sci.* 1991;49:PL223–PL228.
36. Powell JS, Clozel JP, Muller RKM, Kuhn H, Hefti F, Hosang M, Baumgartner HR. Inhibitors of angiotensin converting enzyme prevent myointimal proliferation after vascular injury. *Science.* 1989;245:186–188.
37. Dzau VJ, Mann MJ, Morishita R, Kaneda Y. Fusigenic viral liposome for gene therapy in cardiovascular diseases. *Proc Natl Acad Sci U S A.* 1996;93:11421–11425.
38. Kaneda Y, Uchida T, Kim J, Ishiura M, Okada Y. The improved efficient method for introducing macromolecules into cells using HVJ (Sendai virus) liposome with gangliosides. *Exp Cell Res.* 1987;173:56–69.
39. Nakanishi M, Uchida T, Sugawa H, Ishiura M, Okada Y. Efficient introduction of contents of liposome into cells using HVJ (Sendai virus). *Exp Cell Res.* 1985;159:399–409.
41. Leonetti JP, Mechti N, Degols G, Gagnor C, Lebleu B. Intracellular distribution of microinjected antisense oligonucleotides. *Proc Natl Acad Sci U S A.* 1991;88:2702–2706.
42. Chin DJ, Green GA, Zon G, Szoka FC, Straubinger RM. Rapid nuclear accumulation of injected oligodeoxynucleotides. *New Biol.* 1990;2:1091–1100.
43. MERCATOR Study Group. Does the new angiotensin converting enzyme inhibitor cilazapril prevent restenosis after percutaneous transluminal coronary angioplasty? *Circulation.* 1992;86:110–110.
44. MARCATOR Investigators. Angiotensin converting enzyme inhibition and restenosis: the final results of MARCATOR Trial. *Circulation.* 1992;86(suppl I):I-53. Abstract.
45. Urata H, Kinoshita A, Perez DM, Misono KS, Bumpus FM, Graham RM, Husain A. Cloning of the gene and cDNA for human heart chymase. *J Biol Chem.* 1991;266:17173–17179.
46. Shiota N, Okunishi H, Fukamizu A, Sakonjo H, Kikumori M, Nishimura T, Nakagawa T, Murakami K, Miyazaki M. Activation of two angiotensin-generating systems in the balloon-injured artery. *FEBS Lett.* 1993;323:239–242.